J. Am. Chem. Soc. **2000,** *122,* 661−667

Production and IR Absorption of Cyclic CS_2 in Solid Ar

Mohammed Bahou, Yu-Chang Lee, and Yuan-Pern Lee*

Contribution from the Department of Chemistry, National Tsing Hua University, 101, Sec. 2, Kuang Fu Road, Hsinchu, Taiwan 30013

Received June 9, 1999

Abstract: Linear carbon disulfide (denoted as SCS) isolated in solid N_2 or Ar at 13 K was irradiated with light at 193 nm from an ArF excimer laser. In addition to an absorption line of CS at 1277.4 cm^{-1}, new lines at 881.3 and 520.9 cm^{-1} were observed after photolysis of SCS in solid N_2. These lines are assigned to cyclic CS_2 (denoted *cyc*-CS_2) based on results from ^{34}S- and ^{13}C-isotopic experiments. Doublet lines of *cyc*-CS_2 at 876.5 (881.1) and 517.7 (522.7) cm^{-1} were observed after irradiation of SCS in solid Ar at 193 nm; lines in parentheses are associated with a minor matrix site. Secondary photolysis at 248, 308, 532, 560, or 580 nm diminishes signals of *cyc*-CS_2 and produces SCS. Theoretical calculations using MP2-full and density-functional methods (BLYP and B3LYP) predict three isomers of CS_2: SCS, *cyc*-CS_2, and linear CSS; relative energies, structures, vibrational wavenumbers, and IR intensities were predicted for each isomer. *Cyc*-CS_2 has C−S bonds (∼1.74 Å) elongated relative to those of SCS (∼1.56 Å), a S−S bond ∼2.14 Å, and $\angle SCS \approx 76°$; it lies ∼73 kcal mol^{-1} above SCS. Calculated vibrational wavenumbers, IR intensities, and isotopic shifts for *cyc*-CS_2 fit satisfactorily with experimental results. An asymmetric transition state connecting SCS and *cyc*-CS_2 is characterized, yielding a ring-opening barrier of ∼24.4 kcal mol^{-1} (zero-point energy corrected). Photoconversion between linear and cyclic CS_2 in a matrix cage is discussed.

Introduction

Species such as CO_2, OCS, N_2O, ICN, and CS_2 have 16 valence electrons; these triatomic molecules belong to a class that has received much attention, both theoretical and experimental.[1] On the basis of molecular-orbital theory, the most stable conformation of these molecules is found to be linear. Electronic excitation of these species is typically accompanied by a substantial change in geometry, and the low-lying excited-state tends to become angular. For instance, in its first excited singlet state $^1\Sigma_u^+(^1B_2)$ carbon disulfide (denoted SCS) is bent with $\angle SCS \approx 153°$; the C−S bond length increases from 1.557 Å in the ground ($^1\Sigma_u^+$) state to ∼1.66 Å.[2,3] It is generally accepted that angular carbon disulfide is unstable. Cyclic triatomic molecules with 16 valence electrons are also considered highly unstable and hence receive little attention. However, it is conceivable that if the two terminal S atoms of SCS approach each other as the SCS-angle decreases, bonding between two S atoms might occur, resulting in formation of a cyclic (ring) isomer. Although its energy is expected to be greater than that of its linear isomer, a barrier to rearrangement might exist such that spontaneous decomposition at low temperatures might be inhibited. To our knowledge, no observation of cyclic CS_2 (denoted *cyc*-CS_2) is so far reported.

The matrix isolation technique has gained its reputation for trapping and preserving unstable species at low temperature.[4,5] In situ photolysis of a matrix sample has been a simple yet powerful method to produce unstable species. As photofragments tend to be confined within the matrix cage and to react with each other, the possibility to form various isomers of the precursor is much greater than in the gas phase. Application of lasers as photolytic sources enables one to perform selective photolysis and to avoid secondary photolysis of species of interest. Taking advantage of laser photolysis and the matrix cage effect, we produced numerous new species by photolysis of selective precursors in situ.[6−14] Assignments of new lines are based on isotopic experiments and further supported by theoretical calculations. Here we report production and identification of *cyc*-CS_2 from irradiation of matrix-isolated SCS at 193 nm.

Experimental Section

The experimental setup is similar to that described previously.[7,11] The substrate for a cold matrix sample at 13 K was a copper mirror plated with platinum to reflect the infrared beam to a detector. Matrix samples were prepared by depositing a premixed gaseous sample of carbon disulfide (SCS) in argon or in nitrogen onto the matrix support.

---

[*] To whom correspondence should be addressed; jointly appointed by the Institute of Atomic and Molecular Sciences, Academia Sinica, Taipei, Taiwan. Fax: 886-3-5722892. E-mail: yplee@mx.nthu.edu.tw.

(1) Rabalais, J. W.; McDonald, J. M.; Scherr, V.; McGlynn, S. P. *Chem. Rev.* **1971**, *71*, 73−108 and references therein.

(2) Douglas, A. E.; Zanon, I. *Can. J. Phys.* **1964**, *42*, 627−631.

(3) Brasen, G.; Leidecker, M.; Demtröder W.; Shimamoto, T.; Kato, H. *J. Chem. Phys.* **1998**, *109*, 2779−2790.

(4) Clark, R. J. H.; Hester, R. E. Ed. *Spectroscopy of Matrix Isolated Species*; John Wiley & Sons: New York, 1989.

(5) Andrews, L.; Moskovits, M. Ed. *Chemistry and Physics of Matrix-Isolated Species*; North-Holland: New York, 1989.

(6) Lo, W.-J.; Lee, Y.-P. *J. Chem. Phys.* **1994**, *101*, 5494−5499.

(7) Lo, W.-J.; Shen, M.-y.; Yu, C.-h.; Lee, Y.-P. *J. Chem. Phys.* **1996**, *104*, 935−941.

(8) Lo, W.-J.; Lee, Y.-P. *Chem. Phys. Lett.* **1994**, *229*, 357−361.

(9) Lo, W.-J.; Lee, Y.-P.; Tsai, J.-H. M.; Tsai, H.-H.; Hamilton, T. P.; Harrison, J. G.; Beckman, J. S. *J. Chem. Phys.* **1995**, *103*, 4026−4034.

(10) Lo, W.-J.; Lee, Y.-P.; Tsai, J.-H. M.; Beckman, J. S. *Chem. Phys. Lett.* **1995**, *242*, 147−152.

(11) Jou, S.-H.; Shen, M.-y.; Yu, C.-h.; Lee, Y.-P. *J. Chem. Phys.* **1996**, *104*, 5745−5753.

(12) Chen, L.-S.; Lee, C.-I.; Lee, Y.-P. *J. Chem. Phys.* **1996**, *105*, 9545−9460.

(13) Lo, W.-J.; Shen, M.-y.; Yu, C.-h.; Lee, Y.-P. *J. Mol. Spectrosc.* **1997**, *183*, 119−128.

(14) Lee, C.-I.; Lee, Y.-P.; Wang, X.; Qin, Q.-Z. *J. Chem. Phys.* **1998**, *109*, 10446−10455.

10.1021/ja991926d CCC: $19.00

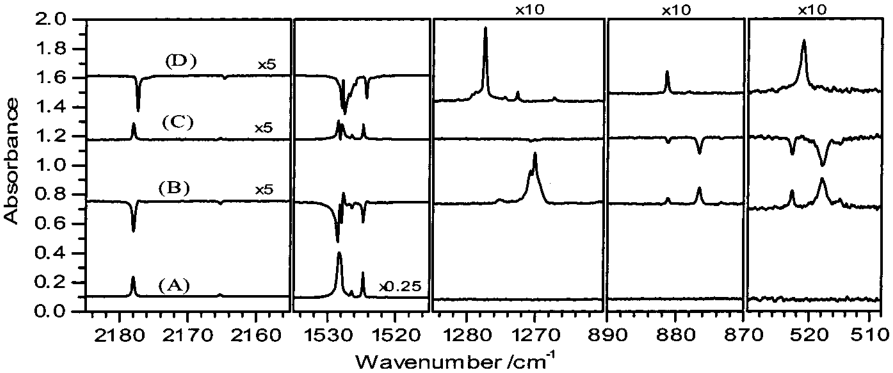

Figure 1. Partial IR absorption spectrum of a SCS/Ar (1/2000) matrix sample before irradiation (A), difference spectrum after irradiation at 193 nm for 2 h (B), difference spectrum after further irradiation at 532 nm for 1 h (C), and difference spectrum of a SCS/N_2 (1/2000) matrix sample after irradiation at 193 nm for 2 h (D). The absorbance scale was expanded 10-fold in the region 1285−510 cm^{-1} and 5-fold (except spectrum A) in the region 2185−2155 cm^{-1}.

Typically 10 mmol of a sample mixture was deposited over a period of 2−3 h. The molar fraction of SCS in argon or nitrogen was typically 1/2000−1/5000.

IR absorption spectra were recorded with a Fourier transform infrared (FTIR) spectrometer (Bomem DA8) equipped with a KBr beam splitter and a Hg/Cd/Te detector (77 K) to cover the spectral range 430−4000 cm^{-1}. Typically 600 scans with resolution of 0.2 cm^{-1} were recorded at each stage of the experiment. The optical path between the FTIR, the cryogenic system, and the detector was purged with nitrogen to avoid atmospheric absorption of H_2O and CO_2.

An ArF excimer laser (193 nm), operated at 10 Hz with energies 2.0−4.0 mJ pulse^{-1}, was employed to photodissociate the matrix sample. Light sources for secondary photolysis include a KrF excimer laser (248 nm), a XeCl laser (308 nm), a frequency-doubled Nd:YAG laser (532 nm), and a tunable dye laser pumped with a Nd:YAG laser to yield emission in a region 560−620 nm (Rhodamine 590 and DCM dyes).

$^{34}SC^{34}S$ (Cambridge Isotope Laboratories, listed isotopic purity of 90%) was used without purification. Scrambled ^{32}S- and ^{34}S-isotopic species was produced in a Pyrex vacuum manifold by mixing $^{32}SC^{32}S$ and $^{34}SC^{34}S$ in equal proportions followed by electric discharge with a tesla coil for a few minutes.

Computational Method

The equilibrium structure, vibrational frequencies, IR intensities, and single-point energies were calculated with the Gaussian 94 program.[15] We used three methods: second-order Moller−Plesset theory[16] employing all active orbitals (MP2-full) and two types of density functional theory (DFT) calculations, BLYP and B3LYP. The BLYP method uses Becke's exchange functional,[17] which includes Slater exchange functional with corrections involving a gradient of the density, and a correlation functional of Lee, Yang, and Parr,[18,19] with both local and nonlocal terms. The B3LYP method uses Becke's three-parameter hybrid exchange functional.[20] The standard 6-31+G* basis set and Dunning's correlation-consistent polarized valence triple-ζ basis set, augmented with *s*, *p*, *d*, and *f* functions (aug-cc-pVTZ) were used in all methods. Analytic first derivatives were utilized in geometry optimization, and vibrational frequencies were calculated analytically at each stationary point.

Results and Discussion

A. Experimental Observations and Assignments. 1. Experiment with SCS in Natural Abundance. The IR spectrum of SCS isolated in solid Ar is well characterized; it exhibits site splitting. Observed lines at 1528.2 (and 1526.4) cm^{-1} (Figure 1, trace A) are consistent with previous report;[21] they are assigned to the asymmetric CS-stretching (ν_3) mode of SCS. Wavenumbers listed in parentheses are associated with a minor matrix site with integrated intensity 0.1% of that of the major site. The symmetric CS-stretching (ν_1, 657.7 cm^{-1} in solid Ar) is IR inactive, and the weak bending (ν_2) mode is reported to lie at 395.1 cm^{-1},[21] outside the spectral range of our experiment. Lines at 2177.9 (and 2177.4) cm^{-1} are assigned as the $\nu_1 + \nu_3$ combination band. Lines observed at 1524.5 (1522.9) and 2165.2 cm^{-1} correspond to the ν_3 and $\nu_1 + \nu_3$ modes of $^{32}SC^{34}S$, respectively. The ratio of integrated intensities of $^{32}SC^{34}S$/$^{32}SC^{32}S$ is ~9.4%, consistent with the natural abundance of the isotopomer $^{32}SC^{34}S$. Very weak lines at 2323.8 (2323.3) and 2825.4 cm^{-1} are assigned to the $2\nu_2 + \nu_3$ and $2\nu_1 + \nu_3$ modes, respectively. Observed wavenumbers of various isotopomers of SCS are listed in Table 1. Integrated intensities of $\nu_1 + \nu_3$, $2\nu_2 + \nu_3$, and $2\nu_1 + \nu_3$ are ~0.026, 0.0022, and 0.0002 of that of ν_3, respectively; absorption of ν_3 might be saturated.

Irradiation of the SCS/Ar (1/2000) matrix with an ArF laser at 193 nm for 2 h produced new lines at 1270.7, 1270.0, 881.1, 876.5, 522.7, and 517.7 cm^{-1} and decreased absorption of lines attributed to SCS, as shown in the difference spectrum in Figure 1, trace B. A positive feature indicates production after irradiation, whereas a negative feature indicates destruction. Approximately 15 ± 5% of SCS was photodissociated. Further irradiation of the matrix sample with laser light at 532 nm from a frequency-doubled Nd:YAG laser for 1h diminished lines at 876.5, 881.1, 517.7, and 522.7 cm^{-1} nearly completely, whereas lines at 1270.7 and 1270.0 cm^{-1} remained unchanged, as illustrated in the difference spectrum in Figure 1, trace C. The photodissociated SCS precursor was recovered to nearly 65 ± 10% of original content after this process.

The line at 1270.0 (1270.7) cm^{-1} is readily assigned to the CS photofragment; the wavenumber is consistent with previous report (1275.4 and 1270.2 cm^{-1}).[22,23] C_2S_2, which has an intense

---

[15] Frisch, M. J.; Trucks, G. W.; Schlegel, H. B.; Gill, P. M. W.; Johnson, B. G.; Robb, M. A.; Cheeseman, J. R.; Keith, T.; Petersson, G. A.; Mongomery, J. A.; Raghavachari, K.; Al-laham, M. A.; Zakrzewski, V. G.; Ortiz, J. V.; Foresman, J. B.; Cioslowski, J.; Stefanov, B. B.; Nanayakkara, A.; Challacombe, M.; Peng, C. Y.; Ayala, P. Y.; Chen. W.; Wong, M. W.; Andres, J. L.; Replogle, E. S.; Gomperts, R.; Martin, R. L.; Fox, D. J.; Binkley, J. S.; Defrees, D. J.; Baker, J.; Stewart, J. P.; Head-Gordon, M.; Gonzalez, C.; Pople, J. A. *Gaussian 94*, revision D3; Gaussian Inc.: Pittsburgh, PA, 1995.

[16] Head-Gordon, M.; Pople, J. A.; Frisch, M. J. *Chem. Phys. Lett.* **1988**, *153*, 503−506.

[17] Becke, A. D.; *Phys. Rev. A.* **1988**, *38*, 3098−3100.

[18] Lee, C.; Yang, W.; Parr, R. G. *Phys. Rev. B.* **1988**, *37*, 785−789.

[19] Miehlich, B.; Savin, A.; Stoll, H.; Preuss, H. *Chem. Phys. Lett.* **1989**, *157*, 200−206.

[20] Becke, A. D. *J. Chem. Phys.* **1993**, *98*, 5648−5652.

[21] Givan, A.; Loewenschuss, A.; Bier, K. D.; Jodl, H. J.; *Chem. Phys.* **1986**, *106*, 151−159.

[22] Bohn, R. B.; Hannachi, Y.; Andrews, L. *J. Am. Chem. Soc.* **1992**, *114*, 6452−6459.

Table 1. Observed Wavenumbers/cm^{-1} of Various Isotopic Species of SCS in Solid Ar and N_2

	$^{32}SC^{32}S$		$^{32}SC^{34}S$		$^{34}SC^{34}S$		$^{32}S^{13}C^{32}S$		$^{32}S^{13}C^{34}S$		$^{34}S^{13}C^{34}S$	
vib. mode	in Ar	in N_2	in Ar	in N_2	in Ar	in N_2	in Ar	in N_2	in Ar	in N_2	in Ar	in N_2
ν_3	1528.2 (1526.4)[a]	1527.8	1524.5 (1522.9)[a]	1524.3	1521.2 (1518.1)[a]	1520.8	1478.4 (1476.4)[a]	1478.0	1474.8 (1472.9)[a]	1474.4	1471.2 (1468.0)[a]	1470.8
$\nu_1 + \nu_3$	2177.9 (2177.4)	2177.4	2165.2	2164.7	2152.4	2151.8	2127.6	2127.2	2115.0	2114.5	2102.1	2101.6
$2\nu_2 + \nu_3$	2323.8 (2323.3)	2326.1	2318.3 (2317.7)	2320.6	2312.8 (2312.2)	2315.1	2248.7	2251.0				
$2\nu_1 + \nu_3$	2825.4	2826.7	2803.7		2781.6		2774.3	2773.8				

[a] Numbers listed in parentheses correspond to a minor matrix site.

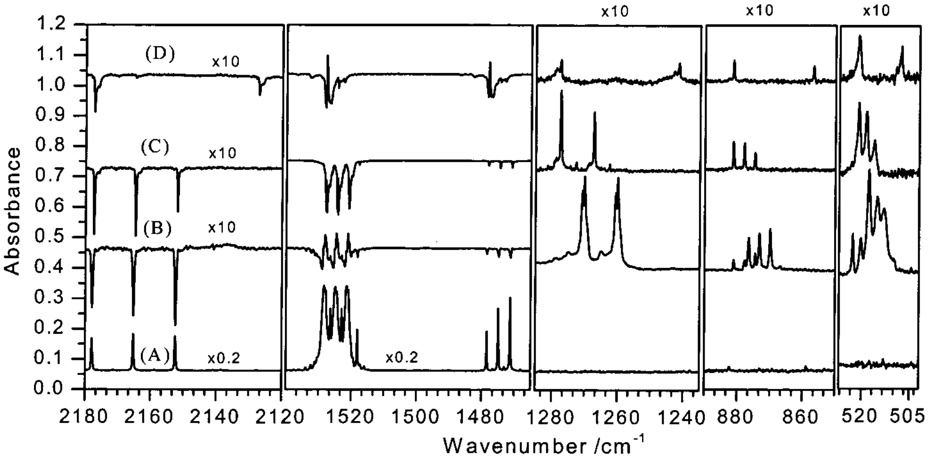

Figure 2. Partial IR absorption spectrum of a ^{32}S-, ^{34}S-scrambled SCS/Ar (1/2000) matrix sample before irradiation (A), difference spectrum after irradiation at 193 nm for 2 h (B), difference spectrum of a ^{32}S-, ^{34}S-scrambled SCS/N_2 (1/2000) matrix sample after irradiation at 193 nm for 2 h (C), and difference spectrum of a $S^{12}CS/S^{13}CS/N_2$ (1/1/2000) matrix sample after irradiation at 193 nm for 1h (D). The absorbance scale was expanded 10-fold in the region 1280−510 cm^{-1} and by factors listed for each spectrum in other regions.

absorption line at 1179 cm^{-1},[22,24] might be formed from dimerization of CS. We did not observe absorption near 1179 cm^{-1}, presumably because the concentration of CS_2 (1/2000) is low and CS does not migrate easily. Lines at 876.5 (881.1) and 517.7 (523.7) cm^{-1} are previously unobserved. The wavenumbers listed in parentheses are associated with a minor site with integrated intensity ~25 ± 3% relative to that of the major site. Observed wavenumbers fail to correspond to those of ionic forms of the precursor such as CS_2^+ (618, 349, 1207 cm^{-1} in solid Ne)[25−28] and CS_2^- (1159.4 cm^{-1} in solid Ne).[29]

Similar experiments were performed for SCS isolated in N_2 (1/2000). Singlet lines at 1527.8 and 2177.4 cm^{-1} were observed before photolysis; they are assigned to ν_3 and $\nu_1 + \nu_3$ modes of $^{32}SC^{32}S$, respectively. Weak lines at 1524.3 and 2164.7 cm^{-1} correspond to $^{32}SC^{34}S$ isolated in solid N_2. After irradiation at 193 nm, CS (1277.4 cm^{-1}, with $C^{34}S$ at 1267.2 cm^{-1}) and two singlet lines at 881.3 and 520.9 cm^{-1} were produced, as shown in Figure 1, trace D. Observation of singlet lines in solid N_2 supports assignments of doublet lines observed in solid Ar to matrix site-splitting.

2. ^{34}S- and ^{13}C-Isotopic Experiments. When a mixture containing $^{32}SC^{32}S$ and $^{34}SC^{34}S$ in nearly equal proportions was deposited with Ar, the IR absorption spectrum shows only lines due to $^{32}SC^{32}S$ (1528.2 and 2177.9 cm^{-1}) and $^{34}SC^{34}S$ (1521.2 and 2152.4 cm^{-1}); lines due to $^{32}SC^{34}S$ (1524.5 and 2165.2 cm^{-1}) are weak (~9% of $^{32}SC^{32}S$). This indicates that S-isotopic scrambling of CS_2 does not occur at room temperature.

A scrambled isotopic mixture containing $^{32}SC^{32}S$, $^{32}SC^{34}S$, and $^{34}SC^{34}S$ in nearly equal proportions was prepared as described in the Experimental Section. A partial IR absorption spectrum of the mixture isolated in solid Ar is shown in Figure 2, trace A. Line positions of each isotopomer of SCS are listed in Table 1. Relative integrated intensities of the $\nu_1 + \nu_3$ line of species are $^{32}SC^{32}S$:$^{32}SC^{34}S$:$^{34}SC^{34}S$ $\simeq$ 1.00:1.12:1.04.

The difference spectrum after irradiation at 193 nm for 2 h is shown in Figure 2, trace B. Line positions of a newly formed species in each isotopic variant are listed in Table 2. The doublet at 876.5 and 881.1 cm^{-1} split into three pairs, with new lines at 873.2 (877.8) and 869.9 (874.6) cm^{-1}. Integrated intensities of lines due to major (minor) isotopic species exhibit a ratio of 1.00:1.18:1:26 (1.00:1.03:1.57), respectively, consistent with that of $\nu_1 + \nu_3$ lines of photodissociated $^{32}SC^{32}S$:$^{32}SC^{34}S$:$^{34}SC^{34}S$ = 1.00:1.38:1.41. The isotopic pattern indicates that two equivalent S atoms are involved in this mode. The isotopic ratios, defined as a ratio of vibrational wavenumbers of the ^{34}S-labeled species to that of the ^{32}S-species, of 873.2/876.5 = 0.9962 and 869.9/876.5 = 0.9925 are similar to, but slightly smaller than, those (1524.5/1528.2 = 0.9976 and 1521.2/1528.2 = 0.9954) of SCS in its ν_3 mode. The doublet at 517.7 and 522.7 cm^{-1} also split into three pairs with overlapped lines. After deconvolution, peak positions of these new lines lie at 514.6 (520.2) and 513.0 (517.7) cm^{-1}; lines associated with the

---

(23) Jacox, M. E.; Milligan, D. E. *J. Mol. Spectrosc.* **1975**, *58*, 142−157.

(24) Maier, G.; Reisenauer, H. P.; Schrot, J.; Janoschek, R. *Angew. Chem., Int. Ed. Engl.* **1990**, *29*, 1464−1466; *Angew. Chem.* **1990**, *102*, 1457−1459.

(25) Bondybey, V. E.; English, J. H.; Miller, T. A. *J. Chem. Phys.* **1979**, *70*, 1621−1625.

(26) Bondybey, V. E.; English, J. H.; Miller, T. A. *J. Chem. Phys.* **1980**, *73*, 3098−3102.

(27) Cheng, B.-M.; Lo, W.-J.; Hung, W.-C. *Chem. Phys. Lett.* **1995**, *236*, 355−361.

(28) Zen, C.-C.; Lee, Y.-P. *Chem. Phys. Lett.* **1995**, *244*, 177−182.

(29) Halasinski, T. M.; Godbout, J. T.; Allison, J.; Leroi, G. E. *J. Phys. Chem.* **1996**, *100*, 14865−14871.

Table 2. Observed Wavenumbers/cm^{-1} of Various Isotopic Species of *Cyc*-CS$_2$ in Solid Ar and N$_2$

	cyc-C^{32}S$_2$		*cyc*-C^{32}S^{34}S		*cyc*-C^{34}S$_2$		*cyc*-^{13}CS$_2$	*cyc*-^{13}C^{34}S$_2$
vib. mode	in Ar	in N$_2$	in Ar	in N$_2$	in Ar	in N$_2$	in N$_2$	in Ar
ν_1	876.5 (881.1)[a]	881.3	873.2 (877.8)[a]	878.0	869.9 (874.6)[a]	874.7	856.8	845.3
ν_3	517.7 (522.7)	520.9	514.6 (520.2)	518.7	513.0 (517.7)	516.1	507.8	499.8

[a] Numbers listed in parentheses correspond to a minor matrix site.

Table 3. Structures and Energies of Three Isomers and a Transition State (TS) of CS$_2$ Predicted with Various Theoretical Methods

species	parameters	MP2-full/ 6-31+G*	MP2-full/ aug-cc-pVTZ	B3LYP/ 6-31+G*	B3LYP/ aug-cc-pVTZ	BLYP/ aug-cc-pVTZ
SCS	*E*/hartrees	−833.29753	−833.56162	−834.49184	−834.57297	−834.53994
	r(C−S)/Å	1.561	1.557	1.563	1.557	1.571
	∠SCS	180°	180°	180°	180°	180°
cyc-CS$_2$	Δ*E*^{a}/ kcal mol^{-1}	86.1	77.3	77.4	73.3	72.8
	r(C−S)/Å	1.719	1.720	1.747	1.739	1.760
	r(S−S)/Å	2.153	2.129	2.151	2.142	2.177
	∠SCS	77.54°	76.48°	76.00°	76.02°	76.40°
CSS	Δ*E*^{a}/kcal mol^{-1}	117.0	103.9	110.0	103.0	96.5
	r(C−S)/Å	1.598	1.585	1.565	1.554	1.578
	r(S−S)/Å	1.903	1.891	1.980	1.957	1.979
	∠CSS	180°	180°	180°	180°	180°
TS^b	ΔE^a/kcal mol^{-1}	108.2			98.0	
	r(C−S$_1$)/Å	1.583			1.577	
	r(C−S$_2$)/Å	1.771			1.779	
	∠CS$_1$S$_2$	41.57°			40.83°	
	∠S$_1$CS$_2$	102.04°			103.73°	

[a] Relative to energy of SCS. [b] Transition state connecting SCS and *cyc*-CS$_2$.

minor site are listed in parentheses. This isotopic pattern also indicates that two equivalent S atoms are involved in this mode. Isotopic ratios of 514.6/517.7 = 0.9940 and 513.0/517.7 = 0.9909 are slightly smaller than for the other band, but within a reasonable range expected for a C−S stretching mode. Observed wavenumbers ∼520 cm^{-1} are greater than those expected for a bending motion, suggesting that this mode is likely associated with asymmetric CS-stretch, whereas lines near 880 cm^{-1} are associated with symmetric CS-stretch. The isotopic ratio for lines due to CS, C^{34}S/C^{32}S = 1259.9/1270.0 = 0.9920, is identical to the theoretical value of 0.9919 for diatomic CS.

The ^{34}S-isotopic experiments in solid N$_2$ clearly show production of isotopic triplets after irradiation of isotopically scrambled SCS at 193 nm, as illustrated in Figure 2, trace C. The line positions listed in Table 2 yield isotopic ratios of 878.0/881.3 = 0.9963, 874.7/881.3 = 0.9925 and 518.7/520.9 = 0.9958, 516.1/520.9 = 0.9908, similar to those observed in solid Ar. The isotopic ratio for C^{34}S, 1267.2/1277.4 = 0.9920, is identical to the theoretical value.

The experiment using a mixed sample of S^{12}CS and S^{13}CS in solid N$_2$ shows production of isotopic doublets after irradiation at 193 nm, as illustrated in trace D of Figure 2. The isotopic pattern indicates that only one C atom is involved in these two modes. The line positions listed in Table 2 yield isotopic ratios of 856.8/881.3 = 0.9722 and 507.8/520.9 = 0.9749, as expected for modes associated with CS stretching. The isotopic ratio for ^{13}CS, 1241.5/1277.4 = 0.9719 is nearly identical to the theoretical value of 0.9716.

Because one C atom and two equivalent S atoms are involved in observed vibrational modes, the new species must be CS$_2$ in either angular or cyclic forms. Observation of small wavenumbers (∼876.5 cm^{-1}) relative to those of SCS (1528.2 cm^{-1}) and CS (1270.0 cm^{-1}) indicates a weak C−S bond, consistent with expectation for *cyc*-CS$_2$. Upon close inspection, we found weak lines at 845.3 and 499.8 cm^{-1} (in Ar) ascribable to new species produced after irradiation of ^{34}S^{13}C^{34}S. For triatomic molecules (XY$_2$) with C_{2v} symmetry, shifts in ν_3 vibrational wavenumbers upon isotopic substitution of central (X) and terminal (Y) atoms lead to lower and upper limits of the bond angle, respectively. Assuming C_{2v} symmetry for the new species and assuming observed lines ∼520 cm^{-1} are associated with asymmetric CS-stretch (ν_3), ν_3 lines from isotopomers 34−12−34 and 34−13−34 yield a lower limit of 74° for the bond angle and those from isotopomers 32−12−32 and 34−12−34 yield an upper limit of 81°; the average value of 77° ± 4° is expected to be a reliable estimate of the bond angle. This small angle indicates that the new species is *cyc*-CS$_2$. *Hence, we conclude that new lines at 876.5 (881.1) and 517.7 (522.7) cm^{-1} belong to* cyc-*CS$_2$ isolated in solid Ar, and lines at 881.3 and 520.9 cm^{-1} belong to cyc-CS$_2$ isolated in solid N$_2$.*

B. Comparison with Theoretical Calculations. We performed a series of high-level ab initio calculations using MP2-full, BLYP, and B3LYP methods to find three stable isomers of CS$_2$: linear SCS, *cyc*-CS$_2$, and linear CSS. The geometries and energies predicted for these species are listed in Table 3. The structures of these isomers predicted with B3LYP/aug-cc-pVTZ are illustrated in Figure 3. Use of the aug-cc-pVTZ basis set decreases slightly the energies of *cyc*-CS$_2$ and CSS relative to SCS. Both MP2-full and B3LYP methods (with aug-cc-pVTZ basis sets) predict a C−S bond length (1.557 Å) of SCS nearly identical to the experimental value of 1.5549 ± 0.004 Å,[30] whereas the BLYP method predicts a slightly greater value of 1.571 Å.

The *cyc*-CS$_2$ isomer is characterized by a small SCS angle ∼76° and a relatively long C−S bond (∼1.74 Å), compared with those of SCS (1.557 Å) and CSS (∼1.57 Å). The S−S bond length ∼2.14 Å of *cyc*-CS$_2$ is greater than that of S$_2$ (∼1.889 Å)[31] or HSSH (2.055 Å).[32] The energy of *cyc*-CS$_2$ lies

---

(30) Kolbuszewski, M.; Bunker, P. R.; Jensen, P. *J. Mol. Spectrosc.* **1995**, *170*, 158−165.

(31) Huber, K. P., Herzberg, G., Eds. *Constants of Diatomic Molecules*; Van Norstrand Reinhold: New York, 1979.

Table 4. Vibrational Wavenumbers/cm^{-1} and Infrared Intensities of Three Isomers of CS_2 Predicted with Various Theoretical Methods

species	vib. mode	MP2-full/ 6-31+G*	B3LYP/ 6-31+G*	B3LYP/ aug-cc-pVTZ	BLYP/ aug-cc-pVTZ
SCS	ν_1, *s*-CS stretch	685.1 (0)[a]	672.8 (0)[a]	673.8 (0)[a]	645.4 (0)[a]
	ν_2, SCS bend	389.6 (5.1)	404.0 (2.4)	403.0 (3.6)	383.5 (4.1)
	ν_3, *a*-CS stretch	1634.9 (554)	1550.5 (665)	1551.0 (684)	1501.0 (525)
cyc-CS_2	ν_1, *s*-CS stretch	950.3 (28.8)	886.4 (31.2)	888.5 (21.4)	834.9 (18.6)
	ν_2, SS stretch	477.4 (0.1)	491.4 (0.01)	497.7 (0.01)	464.9 (0.01)
	ν_3, *a*-CS stretch	543.7 (145)	525.8 (112)	511.7 (93.9)	501.4 (81.1)
CSS	ν_1, CS stretch	974.8 (30.1)	1194.0 (10.8)	1214.9 (14.7)	1131.7 (3.5)
	ν_2, CSS bend	89.9 (1.5)	108.3*i* (0.09)	86.3 (0.05)	120.6 (0.00)
	ν_3, SS stretch	637.6 (66.3)	490.9 (32.6)	520.8 (38.1)	502.6 (32.6)

[a] IR intensities (in km mol^{-1}) are listed in parentheses.

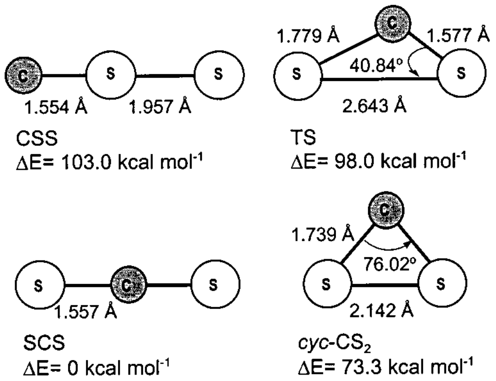

Figure 3. Geometries and relative energies of SCS, *cyc*-CS_2, CSS, and a transition state (TS) connecting SCS and *cyc*-CS_2 calculated with B3LYP/aug-cc-pVTZ method.

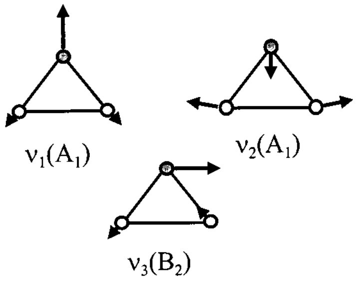

Figure 4. Displacement vector diagrams of three vibrational modes of *cyc*-CS_2 calculated with B3LYP/aug-cc-pVTZ method. Corresponding symmetry is listed in parentheses.

~73 kcal mol^{-1} above that of SCS, but ~24−30 kcal mol^{-1} below that of CSS.

Table 4 lists vibrational wavenumbers and infrared intensities (in parentheses) predicted for three isomers of CS_2 with various methods. Both B3LYP and BLYP predict similar vibrational wavenumbers for SCS, with the former nearly identical to experimental values ($\omega_1 = 672.7$, $\omega_2 = 398.2$, $\omega_3 = 1558.7$ cm^{-1}) in the gas phase.[33−35] Observed wavenumbers of new lines (876.5 and 517.7 cm^{-1} in Ar and 881.3 and 520.9 cm^{-1} in N_2) are near values predicted for ν_1 (symmetric CS-stretch) and ν_3 (asymmetric CS-stretch) modes (888.5 and 511.7 cm^{-1}) of *cyc*-CS_2 with the B3LYP method; the BLYP method predicts values slightly (<6%) smaller than those of B3LYP, but within expected uncertainties. Displacement vector diagrams of three vibrational modes of *cyc*-CS_2 calculated with B3LYP are shown in Figure 4. The ratio of integrated intensities between observed lines at 876.5 and 517.7 cm^{-1}, 0.25 ± 0.05, is also consistent with that (~0.23) predicted with both B3LYP and BLYP methods. IR absorption of the ν_2 mode (mainly SS-stretch) of *cyc*-CS_2 is predicted to be extremely weak.

Predicted isotopic ratios typically show small errors even when predicted vibrational wavenumbers deviate from experimental results by a relatively large fraction. Table 5 lists predicted ^{34}S- and ^{13}C-isotopic ratios of three isomers. Both B3LYP and BLYP methods predict near identical isotopic ratios for SCS which are nearly the same as those determined experimentally (deviation < 0.22%). Similarly, predicted ratios of *cyc*-CS_2 agree satisfactorily with experimental values of new lines with deviations less than 0.1% except for ν_3 of *cyc*-$^{13}CS_2$ (deviation 0.65% for B3LYP). *Hence, theoretical calculations also support assignments of lines observed at 876.5 and 517.7 cm^{-1} (in solid Ar) and 881.3 and 520.9 cm^{-1} (in solid N_2) to ν_1 and ν_3 modes of cyc-CS_2.*

Predicted IR absorption lines of CSS lie in regions 1100−1250 cm^{-1} (ν_1) and 500−520 cm^{-1} (ν_3). Although we searched carefully these regions we found no evidence of absorption lines likely assignable to CSS.

Gutsev et al.[36] characterized the potential energy curve and C−S bond length of CS_2 in C_{2v} symmetry for ∠SCS ranging *100−180*° with the CCSD(T)/6-311+G(2*df*) method; they did not find evidence of the existence of *cyc*-CS_2. We performed similar calculations with the B3LYP/aug-cc-pVTZ method to cover ∠SCS in the range 60−180°. Although we could locate *cyc*-CS_2 at ∠SCS $\simeq$ 76°, no transition state between SCS and *cyc*-CS_2 can be characterized if both C−S bond lengths are constrained to be identical (hence the C_{2v} symmetry is maintained). Figure 5A shows a potential energy curve with $r_{CS} = 1.557$ Å and varied ∠SCS. The transition state is located at 98 kcal mol^{-1} above SCS when we lift the C_{2v} symmetry. The geometry of the transition state (TS) is shown in Figure 3 with parameters listed in Table 3. It has an asymmetric shape with two C−S bonds of 1.577 and 1.779 Å, respectively, and ∠SCS = 103.7°. Calculated vibrational frequencies for the transition states are 997.8, 627.3, and 832.2*i* cm^{-1}. When we perform calculations on the reaction path from the transition state using the internal reaction coordinate (IRC) method,[37,38] a smooth transition from SCS to *cyc*-CS_2 is observed, as shown in Figure 5B. The barrier height for ring-opening of *cyc*-CS_2 is thus calculated to be 24.8 kcal mol^{-1}, large enough to allow observation of *cyc*-CS_2 in a low-temperature matrix. With

---

(32) Winnewisser, G.; Winnewisser, M.; Gordy, W. *J. Chem. Phys.* **1968**, *49*, 3465−3478.

(33) Bernath, P. F.; Dulick, M.; Field, R. W.; Hardwick, J. L. *J. Mol. Spectrosc.* **1981**, *86*, 275−285.

(34) Blanquet, G.; Baeten, E.; Cauuet, I.; Walrand, J.; Courtoy, C. P. *J. Mol. Spectrosc.* **1985**, *112*, 55−70.

(35) Cheng, C.-L. C.; Hardwick, J. L.; Dyke, T. R. *J. Mol. Spectrosc.* **1996**, *179*, 205−218.

(36) Gutsev, G. L.; Bartlett, R. J.; Compton, R. N. *J. Chem. Phys.* **1998**, *108*, 6756−6762.

(37) Gonzalez, C.; Schlegel, H. B. *J. Chem. Phys.* **1989**, *90*, 2154−2161.

(38) Gonzalez, C.; Schlegel, H. B. *J. Phys. Chem.* **1990**, *94*, 5523−5527.

Table 5. Isotopic Ratios[a] of Vibrational Wavenumbers of SCS, *Cyc*-CS_2, and CSS Predicted with Various Theoretical Calculations

vib. mode	species	BLYP/ aug-cc-pVTZ	B3LYP/ aug-cc-pVTZ	expt
ν_1	$^{32}S^{12}C^{34}S$	0.9851	0.9851	0.9853[b]
	$^{34}S^{12}C^{34}S$	0.9702	0.9702	0.9700
	$^{32}S^{13}C^{32}S$	0.9984	0.9984	0.9988
ν_2	$^{32}S^{12}C^{34}S$	0.9977	0.9977	0.9974
	$^{34}S^{12}C^{34}S$	0.9953	0.9953	0.9953
	$^{32}S^{13}C^{32}S$	0.9674	0.9667	0.9674
ν_3	$^{32}S^{12}C^{34}S$	0.9977	0.9977	0.9977[c]/0.9977[d]/0.9976[e]
	$^{34}S^{12}C^{34}S$	0.9953	0.9953	0.9954/0.9946/0.9954
	$^{32}S^{13}C^{32}S$	0.9652	0.9663	0.9674/0.9672/0.9674
ν_1	*cyc*-$^{32}S^{12}C^{34}S$	0.9963	0.9962	0.9962[c]/0.9962[d]/0.9963[e]
	cyc-$^{34}S^{12}C^{34}S$	0.9926	0.9924	0.9925/0.9926/0.9925
	cyc-$^{32}S^{13}C^{32}S$	0.9681	0.9706	-/- /0.9722
ν_2	cyc-$^{32}S^{12}C^{34}S$	0.9863	0.9861	
	cyc-$^{34}S^{12}C^{34}S$	0.9728	0.9725	
	cyc-$^{32}S^{13}C^{32}S$	0.9967	0.9936	
ν_3	cyc-$^{32}S^{12}C^{34}S$	0.9953	0.9955	0.9940[c]/0.9952[d]/0.9958[e]
	cyc-$^{34}S^{12}C^{34}S$	0.9903	0.9901	0.9909/0.9904/0.9908
	cyc-$^{32}S^{13}C^{32}S$	0.9593	0.9684	-/- /0.9749
ν_1	$^{12}C^{32}S^{34}S$	0.9999	0.9999	
	$^{12}C^{34}S^{32}S$	0.9906	0.9907	
	$^{12}C^{34}S^{34}S$	0.9905	0.9906	
	$^{13}C^{32}S^{32}S$	0.9721	0.9733	
ν_2	$^{12}C^{32}S^{34}S$	0.9971	0.9970	
	$^{12}C^{34}S^{32}S$	0.9854	0.9852	
	$^{12}C^{34}S^{34}S$	0.9824	0.9822	
	$^{13}C^{32}S^{32}S$	0.9814	0.9807	
ν_3	$^{12}C^{32}S^{34}S$	0.9830	0.9829	
	$^{12}C^{34}S^{32}S$	0.9922	0.9921	
	$^{12}C^{34}S^{34}S$	0.9749	0.9748	
	$^{13}C^{32}S^{32}S$	0.9974	0.9952	

[a] Defined as the ratio of vibrational wavenumbers of a ^{34}S-isotopomer to that of the corresponding $C^{32}S_2$ species. [b] Based on ω_i values in the gas phase; refs 33−35. [c] Based on ν_i values in solid Ar, major site. [d] Based on ν_i values in solid Ar, minor site. [e] Based on ν_i values in solid N_2.

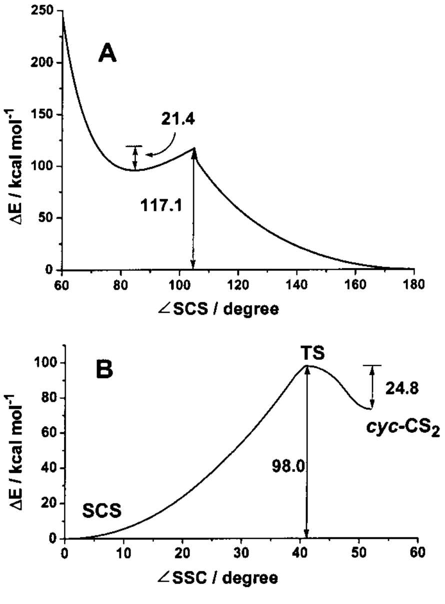

Figure 5. Potential energy curve of CS_2 calculated with the B3LYP/aug-cc-pVTZ method. (A) in C_{2v} symmetry with $r_{CS} = 1.557$ Å and varied ∠SCS, (B) IRC calculation from the transition state. The transition state (TS) is located at 98.0 kcal mol^{-1} above SCS, and *cyc*-CS_2 is 73.3 kcal mol^{-1} above SCS with ∠SCS = 76° (∠SSC = 52°). Values do not include zero-point energies.

corrections of zero-point energies, the transition state lies 96.0 kcal mol^{-1} above SCS and the ring-opening barrier for *cyc*-CS_2 is 24.4 kcal mol^{-1}.

C. Formation mechanism of *cyc*-CS_2. Several authors investigated photolysis of SCS in the UV region.[39−42] Photodissociation at 193 nm proceeds via the $^1\Sigma_u^+(^1B_2)$ surface which leads to predissociation into CS and S:

$$\mathrm{SCS} + 193\ \mathrm{nm} \rightarrow \mathrm{CS}\ (^1\Sigma^+) + \mathrm{S}(^1\mathrm{D}) \qquad (1a)$$

$$\rightarrow \mathrm{CS}\ (^1\Sigma^+) + \mathrm{S}(^3\mathrm{P}) \qquad (1b)$$

for which excess energies are 18.6 and 45 kcal mol^{-1} for reaction 1a and 1b, respectively. The branching ratio between singlet and triplet channels was determined to be $S(^3P)/S(^1D) = 2.8 \pm 0.3$.[40] The energy release in each channel has a similar pattern, with a vibrationally inverted CS fragment having internal energy ~50% of available energy. In a matrix, $S(^1D)$ atoms relax readily to form $S(^3P)$. Observation of absorption lines of CS at 1270.0 and 1270.7 cm^{-1} provides direct evidence for reaction 1; the broad line width indicates that CS might be perturbed by a nearby S atom. The exothermicity of the reverse reaction of 1b, $\Delta H = -105.2$ kcal mol^{-1}, to form SCS indicates that formation of *cyc*-CS_2 (lying ~73 kcal mol^{-1} above SCS) from fragments CS and $S(^3P)$ is thermodynamically feasible

$$\mathrm{S}(^3\mathrm{P}) + \mathrm{CS}\ (^1\Sigma^+) \rightarrow \mathrm{SCS}\ (\mathrm{X}^1\Sigma_g^+) \qquad (2a)$$

$$\rightarrow cyc\text{-}\mathrm{CS}_2\,(\mathrm{X}^1\Sigma) \qquad (2b)$$

Cyc-CS_2 in its electronic ground state, a singlet, does not correlate directly with $S(^3P)$ + CS $(^1\Sigma^+)$. Formation of *cyc*-CS_2 might proceed either via a triplet surface followed by relaxation or via direct rearrangement of excited SCS, with the latter less likely.

When a sample irradiated at 193 nm to produce *cyc*-CS_2 was irradiated further at 248, 308, 532, 560, or 580 nm, lines ascribed to *cyc*-CS_2 become diminished and lines of SCS increase, whereas irradiation at 600 or 620 nm results in no change. This observation indicates that *cyc*-CS_2 either photodissociates to CS + S or isomerizes to SCS readily at $\lambda < 600$ nm; if photodissociation takes place, subsequent recombination favors formation of SCS.

Observation of *cyc*-CS_2 may have important implications. The predicted energy of *cyc*-CS_2 is close to several electronically excited states of SCS. Interaction of *cyc*-CS_2 with these states may be the cause of reported complex UV spectra which remain to be understood.[43] Hence, *cyc*-CS_2 may play an important role in photochemistry of SCS. Extensive theoretical calculations to explore excited electronic surfaces of SCS and *cyc*-CS_2 are in progress.

Conclusions

We photolyzed SCS isolated in solid Ar or N_2 with an ArF excimer laser at 193 nm and observed IR absorption lines at 876.5 (881.1) and 517.7 (522.7) cm^{-1} (in solid Ar, wavenumbers listed in parentheses are associated with a minor matrix site) or 881.3 and 520.9 cm^{-1} (in solid N_2). They are attributed to symmetric CS-stretching (ν_1) and asymmetric CS-stretching (ν_3) modes of *cyc*-CS_2, respectively. Assignments and an estimated

---

(39) Breckenridge, W. H.; Taube, H. *J. Chem. Phys.* **1970**, *53*, 1750−1767.

(40) Waller, I. M.; Hepburn, J. W. *J. Chem. Phys.* **1987**, *87*, 3261−3268.

(41) Mank, A.; Starrs, C.; Jego, M. N.; Hepburn, J. W. *J. Chem. Phys.* **1996**, *104*, 3609−3619.

(42) Dornhöfer, G.; Hack, W.; Langel, W. *J. Phys. Chem.* **1984**, *88*, 3060−3069.

(43) Brasen, G.; Leidecker, M.; Demtröder, W.; Shimamoto, T.; Kato, H. *J. Chem. Phys.* **1998**, *109*, 2779−2790 and references therein.

SCS bond angle of 77 ± 4° are derived based on observed ^{34}S- and ^{13}C-isotopic shifts. Theoretical predictions of line positions, infrared intensities, and $^{34}S/^{32}S$ isotopic ratios of *cyc*-CS_2 agree satisfactorily with experiments. The B3LYP/aug-cc-pVTZ method predicts that *cyc*-CS_2 lies ~73 kcal mol^{-1} above SCS, and that the transition state connecting these two species is asymmetric and lies 98 kcal mol^{-1} above SCS. This work demonstrates an advantage of the matrix-isolation technique to produce and to identify novel isomers that are difficult to generate in the gas phase. *Cyc*-CS_2 may play an important role in photochemistry and spectroscopy of SCS.

Acknowledgment. We thank the National Science Council of the Republic of China for financial support (Contract No. NSC 88-2119-M-007-001)

JA991926D